(R 79 0058H

DETERMINATION OF ^{40}Ca AND ^{48}Ca MATTER DENSITIES BY 600 MeV AND 1 GeV PROTON ELASTIC SCATTERING

I. BRISSAUD and X. CAMPI[*]

Institut de Physique Nucléaire, BP 1, 91406 ORSAY France

Abstract : The 600 MeV and 1 GeV data of proton elastic scattering on $^{40, 48}$Ca have been analyzed in the framework of the Glauber model. The matter distributions are extracted from the data in an approximately model-independent form based on a Fourier series expansion. A similar method is used to deduce directly the ^{48}Ca-^{40}Ca neutron density difference.

IPNO-TH-79-11   February 1979

---

[*]Division de Physique Théorique, Laboratoire associé au C.N.R.S.

Recent proton-nucleus elastic scattering experi-. ments at intermediate energies have revealed the general correctness of theoretical descriptions based on multiple-scattering models. The information obtained from these experiments on the nuclear properties has been somewhat disappointing and in particular the study of neutron distribution of nuclei has been marked by some confusion. This is due to several reasons. First, none of the current theories for hadron-nucleus scattering are believed to be reliable at a momentum transfer higher than $q_{max} = 2-2.5$ fm^{-1}. Beyond this limit higher-order multiple scattering and other complex processes (e.g. rescattering on intermediate states) are important, which implies immediately that details of the density cannot be extracted from these data. Therefore, shell structure oscillations and fine surface details, clearly seen by electron scattering for the charge densities, are washed out for neutron densities, despite the small wave length of the incident protons. Secondly the strong absorption of protons by the nuclear medium prevents an accurate exploration of the interior of the nucleus. The nucleon-nucleon elementary amplitude being a function of the energy, the penetration of a complex nucleus by the incoming protons will depend on the energy, and it is not true that the higher the bombarding energy, the greater will be the penetration of the projectile into the interior of the nucleus. This is one of the points we will briefly examine in this letter. Another source of controversy in the interpretation of these experiments has been motivated by the use, with few exceptions [1,2] , of specific functional forms for the assumed neutron densities. These forms impose an implicit coupling between the tail, the surface region and the interior of the

densities that has no theoretical justification. Consequently, previous analyses have not included a sufficiently detailed or thorough investigation of the many possible sources of indeterminacy which affect the derived neutron densities.

Other methods of greater reliability have been introduced for electron scattering [3,4] , which greatly reduce the model dependence of the experimental analyses and allow for a more complete exploration of the family of densities compatible with experiment. In this letter we apply one of these methods to analyse proton elastic scattering data on ^{40}Ca [5,6] and ^{48}Ca [6] at incident energies of 600 MeV and 1 GeV.

Following the method developed in reference [4] we divide the neutron density into two parts $\rho_n(r) = \rho_0(r) + \rho_1(r)$ where $\rho_0(r)$ is normalized to the correct number of neutrons but otherwise arbitrary (it could be a Fermi function or a calculated Hartree-Fock neutron density). To this is added a correction $\rho_1(r)$, which is expressed as a truncated Fourier series

$$\rho_1(r) = \sum_{m=1}^{L} \frac{2\beta_m}{rR} \sin\left(\frac{m\pi r}{R}\right) \quad 0 < r < R \tag{1}$$

and is zero for $r > R$. The outer radius of this correction is chosen at the outer edge of the density, where the density is small and in fact the error in its determination becomes comparable with ρ_0. The coefficients β_m satisfy one constraint $\sum_{m=1}^{L} (-1)^m \beta_m/m = 0$ to ensure a zero norm for $\rho_1(r)$. The maximum number of coefficients L which can be determined in $\rho_1(r)$ is a function of the maximum momentum transfer used in the analysis. The coefficients β_m are determined by minimizing the mean square error between the experimental data and the calculated differential

cross sections. Throughout this work use is made of the Glauber multiple scattering approximation in its optical limit. The form factor is calculated from the assumed spherically symmetric density

$$F(q) = F_0(q) + \sum_{m=1}^{L} \frac{\beta_m}{q} I_m(q) \tag{2}$$

where $F_0(q)$ is the Fourier transform of $\rho_0 + \rho_p$, ρ_p being the proton density, and

$$I_m(q) = (-1)^m \sin qR \left\{ \frac{2m\pi}{(qR)^2 - (m\pi)^2} \right\} \tag{3}$$

The phase shifts are also linear in the coefficients β_m ,

$$\chi(b) = \chi_0(b) + \sum_m \beta_m \chi_m(b)$$
$$\chi_0(b) = \frac{A}{K_0} \int F_0(q) A(q) J_0(qb) q dq \tag{4}$$
$$\chi_m(b) = \frac{A}{K_0} \int I_m(q) A(q) J_0(qb) dq$$

while the nucleon-nucleus scattering amplitude is not,

$$T(q) = iK \int J_0(qb) [1 - e^{i\chi(b)}] \, bdb \tag{5}$$

In the above formula A is the target mass, K and K_0 being respectively the incident proton momentum in the proton-nucleus and in the proton-nucleon center of mass systems.

We linearize eq.(5) by expanding to first order the exponential, giving

$$T(q) = T_0(q) + \sum_{m=1}^{L} \beta_m T_m(q) \tag{6}$$

with $T_m(q) = K \int J_0(qb) e^{i\chi_0(b)} \chi_m(b) \, bdb$. The coefficients β_m are then determined by a rapidly convergent iterative procedure [4,7] . At the end of each iteration (i) the correction $\rho_i^i (r)$ is added to $\rho_0^i(r)$ to define a new "guess" density $\rho_0^{i+1}(r)$.

At the beginning of the interaction the linearization may not be very accurate, but this is not important since eq.6 is used only to estimate the way to improve the density. When convergence is reached, eq.6 is exact because $\rho_1(r)$ is negligeable. In this way the differential cross section appears as a linear function of β_m and the $\chi^2 = \sum_N \left| \frac{\sigma_{exp}^i - \sigma_{th}^i}{\Delta\sigma_{exp}^i} \right|^2$ can be minimized at each iteration by inverting a matrix as explained in ref. [7]. This method is much faster than the trial and error method used in ref.[1] . The matrix procedure determines both the coefficients β_m and their mean square error, related to the purely statistical error of the experimental data. These errors can be transformed into real space [4,7] and provide a statistical error envelope for the fitted neutron density.

In the formulation above some details of the multiple scattering theory were omitted in order to simplify the presentation. In the actual calculation, however, the complete formulas, given for instance in ref. [8], have been used. The pp and pn scattering amplitudes used are of the form $f(q) = A(q) + C(q) \cdot \vec{\sigma}.\vec{n}$, where the central and spin-orbit terms are given in table I. These values are obtained from a fit of medium energy p-^{4}He scattering data [9]. The contribution of target protons to the scattering has been included in $F_0(q)$, where the protons densities are assumed to be known from elastic electron scattering [10,11]. The effects of finite proton size, electro-magnetic neutron form factor and electromagnetic spin-orbit coupling [12] have been eliminated from the experimental charge densities and the contribution of the Coulomb force has been calculated as in ref.[13].

In the present analyses we have used 94 data points for ^{40}Ca at 600 MeV ($q_{max} \simeq 2.07$ fm^{-1}) [5] , 39 at 1040 MeV ($q_{max} \simeq 2.15$ fm^{-1}) [5] and 35 for ^{48}Ca at 1000 MeV ($q_{max} \simeq 2.10$ fm^{-1}) [6] . The results we have obtained for the matter densities $\rho_m(r) = \rho_p(r) + \rho_n(r)$ of ^{40}Ca and ^{48}Ca are summarized in figure 1. The shaded areas indicate the envelope of the different trial densities which give an agreement with the N experimental data with $\chi^2/N \leq 5$. This upper bound of acceptable densities is somewhat arbitrary and is fixed according to the best fit that can be obtained with conventional 3-parameters Fermi functions used as trial densities. The shaded area is generated by changing R and L in the series of eq. 1 within large bounds ($6 \leq R \leq 14$ fm and $5 \leq L \leq 10$). The figure shows clearly that the density is not determined in the nuclear interior. This insensitivity is mainly due to the absorption of the projectile. This may be seen by comparing the uncertainty envelope for ^{40}Ca at 600 MeV to that at 1 GeV, which follows the trend of the absorptive part of the elementary NN amplitude (see table I). The lack of data at $q > q_{max}$ also contributes to the absolute error envelope but is not relevant for this relative comparison because we have used about the same q_{max} for the two energies. Also drawn in the middle of the error envelope in fig.1a is a typical density surrounded by the purely experimental statistical uncertainties. This is in marked contrast to the electron scattering analysis of proton density distributions. In p-nucleus scattering (except in the surface region) the indetermination arising from experimental uncertainties is much smaller than the one produced by the absorption.

Another question of interest is how the best fit reached with our method compares with those obtained using standard 3-parameter Fermi functions. This point is displayed in fig. 2 where we have plotted the percent error between the experimental $\sigma_{ex}(\theta)$ and calculated $\sigma_{calc}(\theta)$ differential cross sections as a function of the angle, for a sample of our densities and for the best 3-parameters Fermi density. It is clearly seen that the first one is statistically compatible with the experimental data $(\chi^2/N \approx 0.9)$, which is not the case for the optimum Fermi distribution $(\chi^2/N = 5)$.

The error envelopes we found for the matter density of ^{40}Ca are similar to those determined in ref. [1] and [14], where the SOG method of Sick [3] was applied to the analysis of 1 GeV proton scattering data and to 166 MeV α-scattering data respectively. In a similar context, in refs.[15,16] a Fourier series technique was used to calculate the optimum optical potential that reproduced the measured α-scattering cross sections at 104 MeV. In this analysis [16] the matter density was defined with a narrow uncertainties envelope. In comparison with p-scattering, in α-scattering the strong absorption is compensated by the large momentum transfer data that can be included in the analysis ($q \lesssim 5$ fm^{-1} in ref.[15]).

The matter density of ^{48}Ca calculated from the 1 GeV data is shown in figure 1b. It should be noted that the error envelope is smaller than the corresponding one for ^{40}Ca. This feature could be explained by the greater proton penetration in ^{48}Ca than in ^{40}Ca because of the neutron excess in the surface region of ^{48}Ca and $\sigma_{pn}^{tot} < \sigma_{pp}^{tot}$.

Figure 1c shows the neutron excess $\Delta\rho_n = \rho_n^{48} - \rho_n^{40}$. In this analysis we have minimized the source of uncertainties by applying the above technique directly to the difference $\Delta\rho_n(r)$. As input we used the measured proton densities [10,11] for ^{40}Ca and ^{48}Ca and the neutrons Hartree-Fock density calculated by Campi and Sprung [17] . This density (G0), drawn in fig.1, was used as a reference density. The neutron difference $\Delta\rho_n(r)$ was optimized by minimizing χ^2 for the difference of cross sections of ^{48}Ca-^{40}Ca on the same footing as before. The particular choice of $^{40}\rho_n(r)$ affects very little the final $\Delta\rho_n(r)$ and the corresponding uncertainty envelope. Our method of analysing the ^{48}Ca-^{40}Ca neutron difference directly is more accurate than if we considered the two nuclei separately. (It should be noted that the negative parts of $\Delta\rho_n(r)$ are not in contradiction with the theoretical predictions of ref.[17] and can be explained by a neutron core polarization effect).

Table II. shows the values of the matter and mention density radii deduced from the present work along with the corresponding errors associated with the uncertainty envelope. The different values of these radii are compatible with those obtained from other analyses [5,6,15,18,19].

We conclude that it is very difficult to extract precise information about the interior part of the neutron density distributions from proton scattering at high energy. The primary explanation is due to the large absorption which is connected to the large values for σ_{NN}^{tot}. A larger momentum transfer range could, in principle, aid in this determination although an improvement in multiple scattering theories at large q would be needed.

It is a pleasure to thank B. Frois for communicating the charge density of ^{40}Ca before publication and E. Rost for a careful reading of the manuscript.

Note added in proof. After completing this work, we received a preprint from L. Ray (LASL) who analysed 0.8 GeV proton elastic scattering data. A KMT multiple scattering analysis similar to our Glauber model was used. However in his error analysis, a restricted set of densities are allowed thus giving an optimistically small error envelope which cannot be directly compared to ours.

References

[1] I. Brissaud and M.K. Brussel, Phys. Rev. C15 (1977) 452

[2] L. Ray, W.R. Coker and G.W. Hoffman, Phys. Rev. C18 (1978) 2641

[3] I. Sick, Nucl. Phys. A218 (1974) 509

[4] J.L. Friar and J.W. Negele, Nucl. Phys. A212 (1978) 93

[5] Report DPh.N.ME 78-1, edited by G. Bruge (Saclay) 1978, and G. Alkhazov et al., Nucl. Phys. 274 (1976) 443

[6] G. Alkhazov et al., Report 218 Gatchina, USSR (1976), and Phys. Lett. 57B (1975) 47

[7] D. Sprung, J. Martorell and X. Campi, Nucl. Phys. A268 (1976) 301

[8] I. Brissaud et al., Phys. Rev. C11 (1975) 1537

[9] J.P. Auger and R. Lombard, to be published and Ann. of Phys. 115 (1978) 442

[10] B. Frois et al., private communication

[11] I. Sick, Phys. Lett. 53B (1974) 15

[12] W. Bertozzi, J.L. Friar, J. Heisenberg and J.W. Negele, Phys. Lett. 41B (1972) 408

[13] R.J. Glauber and G. Matthiae, Nucl. Phys. B21 (1970) 135

[14] I. Brissaud and M.K. Brussel, J. Phys. G. Nucl. Phys.
      3 (1977) 481

[15] E. Friedman et al., Phys. Rev. Lett. 41 (1978) 1220

[16] H. Rebel et al., Contribution to the Second Louvain-Krakow
      Seminar (1978)

[17] X. Campi and D.W.L. Sprung, Nucl. Phys. A194 (1972) 401

[18] S. Shlomo and R. Schaeffer, Report DPh-T- 78-18, Saclay

[19] A. Chaumaux, V. Layly and R. Schaeffer, Ann. of Phys.
      116 (1978) 247.

Table Captions

Table I   Parameters for the nucleon-nucleon amplitudes [9]

$$f(q) = A(q) + C(q) \ \overline{\sigma}.\overline{n} \text{ with}$$

$$A(q) = \frac{K_s\sigma^{tot}}{4\pi} (1+\alpha)e^{-\beta^2q^2/2} \quad \text{and } \alpha = \alpha_0 + \alpha_1 q^2$$

$$C(q) = \frac{K_0\sigma^{tot}}{4\pi} iq \frac{D_s(1+\alpha_s)}{2M} e^{-\beta_s^2q^2/2}$$

Table II   Point-nucleon r.m.s. radii determined in this work
and from : (a) experimental charge densities
(refs.[10,11]) and (b) Hartree-Fock calculation
(ref.[17]).

E_{lab} (MeV)	σ_{pp}^{tot} (fm^2)	σ_{pn}^{tot} (fm^2)	α_{pp}	α_{pn}	$\alpha_{1p} = \alpha_{1n}$	$\beta_{pp}^2 = \beta_{pn}^2$ (fm^2)	D_s	β_s^2 (fm^2)	α_s
610	3.70	3.60	0.21	-0.22	0.08	0.12	2.8	0.35	1.
1040	4.75	3.85	-0.08	-0.41	0.10	0.25	1.5	0.40	0.7

- Table I -

	$\langle r_p^2 \rangle^{1/2}$ (a)	$\langle r_m^2 \rangle^{1/2}$ Present work	$\langle r_n^2 \rangle^{1/2}$ Present work	$\langle r_n^2 \rangle^{1/2} - \langle r_p^2 \rangle^{1/2}$ Present work	H.F. (b)	$^{48}\langle r_n^2 \rangle^{1/2} - ^{40}\langle r_n^2 \rangle^{1/2}$ Present work	H.F. (b)
^{40}Ca	3.40	3.39 ± 0.04	3.38 ± 0.04	-0.02 ± 0.04	-0.04	0.20 ± 0.08	0.25
^{48}Ca	3.41	3.51 ± 0.04	3.58 ± 0.04	0.17 ± 0.04	0.18		

- Table II -

Figure Captions

Fig. 1   a) Point-nucleon matter density of ^{40}Ca with the
uncertainties envelopes determined at two diffe-
rent incident proton energies. In the middle
of the shaded areas a typical density shows the
amplitude of the purely statistical uncertainties.

         b) Uncertainties envelope for ^{48}Ca.

         c) Neutron excess density $\Delta\rho_n = \rho_n^{48} - \rho_n^{40}$. The
dashed line (G-O) represents the result of a
Hartree-Fock calculation (ref.[17]).

Fig. 2   Percent error $(\sigma_{th} - \sigma_{exp} \pm \Delta\sigma_{exp})/(\sigma_{th} + \sigma_{exp} \pm \Delta\sigma_{exp})$
between the experimental and the calculated diffe-
rential cross sections as a function of the
scattering angle θ_{cm}, for the best 3-parameter Fermi
density and for a typical trial density belonging
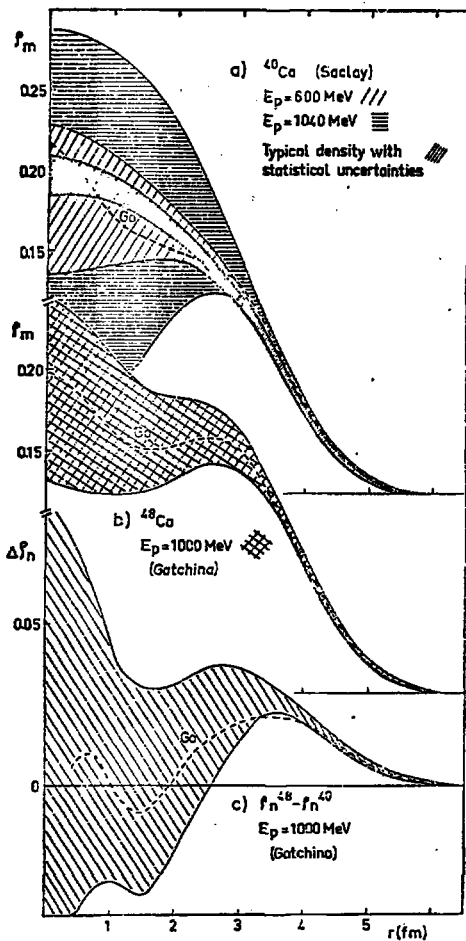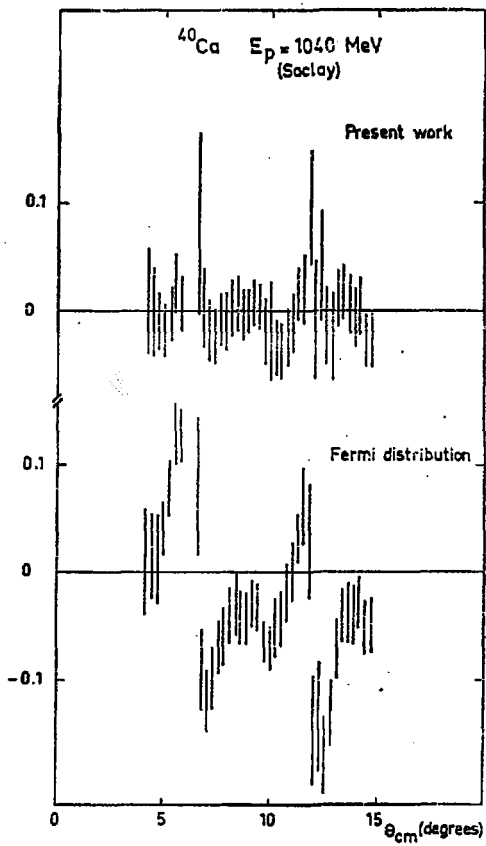to the shaded area of figure 1.

a) ^{40}Ca (Saclay)
$E_p = 600$ MeV ///
$E_p = 1040$ MeV ≡
Typical density with statistical uncertainties ▨

b) ^{48}Ca
$E_p = 1000$ MeV ▨
(Gatchina)

c) $f_n^{48} - f_n^{40}$
$E_p = 1000$ MeV
(Gatchina)

Fig. 1

Fig. 2